DMD Fast Forward. Published on December 28, 2006 as doi:10.1124/dmd.106.013888

Three Dimensional-Quantitative Structure Activity Relationship (3D-QSAR) Analysis Of Human CYP51 Inhibitors

Sean Ekins [1], Dayna C. Mankowski [2], Dennis J. Hoover, Michael P. Lawton, Judith L. Treadway, and H. James Harwood, Jr.

Pfizer Global Research and Development, Groton Laboratories

Eastern Point Rd, Groton, CT 06340 (S.E., D.C.M., D.J.H., M.P.L., J.L.T., H.J.H)

Running title: 3D-QSAR for CYP51 inhibition

Corresponding author: Sean Ekins, D.Sc., Vice President, Computational Biology, ACT LLC, 601 Runnymede Avenue, Jenkintown, PA 19046. Phone 269-930-0974; Fax 215-481-0159; Email ekinssean@yahoo.com

Number of Text pages:	28
Tables:	3
Figures:	3
References:	59
Words in Abstract:	250
Words in Introduction:	865
Words in Discussion:	1497

Abbreviations: CYP, cytochrome P450; 3D-QSAR, 3-dimensional-quantitative structure activity relationship; DTT, dithiothreitol; EDTA, ethylenediamine tetraacetic acid.

ABSTRACT

CYP51 fulfills an essential requirement for all cells, by catalyzing three sequential monooxidations within the cholesterol biosynthesis cascade. Inhibition of fungal CYP51 is used as a therapy for treating fungal infections, while inhibition of human CYP51 has been considered as a pharmacological approach to treat dyslipidemia and some forms of cancer. In order to predict the interaction of inhibitors with the active site of human CYP51, a 3-dimensional quantitative structure activity relationship (3D-QSAR) model was constructed. This pharmacophore model of the common structural features of CYP51 inhibitors was built using the program Catalyst™ from multiple inhibitors (n = 26) of recombinant human CYP51-mediated lanosterol 14α-demethylation. The pharmacophore, which consisted of 1 hydrophobe, 1 hydrogen bond acceptor and 2 ring aromatic features, demonstrated a high correlation between observed and predicted IC_{50} values (r = 0.92). Validation of this pharmacophore was performed by predicting the IC_{50} of a test set of commercially available (n = 19) and CP-320626-related (n = 48) CYP51 inhibitors. Using predictions below 10 μM as a cutoff indicative of active inhibitors, 16 of 19 commercially available inhibitors (84 %) and 38 of 48 CP-320626-related inhibitors (79.2 %) were predicted correctly. In order to better understand how inhibitors fit into the enzyme, potent CYP51 inhibitors were used to build a Cerius^{2} ™ receptor surface model representing the volume of the active site. This study has demonstrated the potential for ligand-based computational pharmacophore modeling of human CYP51 and enables a high-throughput screening system for drug discovery and database mining.

Cytochrome P450 enzymes (CYPs) are a widely studied, large superfamily of heme-thiolate proteins involved in the metabolism of endobiotics and xenobiotics across eukaryotes and prokaryotes (Nelson et al., 1996). The clinical relevance of CYPs is their central role in drug metabolism, which can occur in all human tissues and may be inhibited by the co-administration of competing xenobiotics for the same enzyme (Wrighton et al., 1995). Much less is known about the endogenous functions of P450, although their role in steroid metabolism is an exception. It has been postulated that other endogenous roles might be in neurotransmitter metabolism (Hiroi et al., 1998) and signaling pathways (Chan et al., 1998). One of these enzymes is the ubiquitously expressed CYP51, also known as lanosterol 14 α–demethylase (P450-14DM) (Nelson et al., 1996). This enzyme fulfills an essential requirement for all cells by catalyzing three sequential monooxidations within the cholesterol biosynthesis cascade (Trzaskos et al., 1986; Waterman and Lepesheva, 2005).

CYP51 is one of the most conserved CYPs across phyla (Aoyama et al., 1996; Yoshida et al., 1997), with a 93 % amino acid sequence identity between rat and human and 39-42% identity between mammalian and fungal enzymes (Aoyama et al., 1996; Yoshida et al., 1997). In humans there are three CYP51 genes, including two pseudogenes and a functional gene on chromosome 7 (Rozman et al., 1996). Substrates for CYP51 from mammals, plants and fungi are lanosterol, obtusifoliol and 24-methylene-dihydroxylanosterol, respectively (Lamb et al., 1998). Such substrate specificities can be explained by a limited number of amino acid substitutions in substrate recognition sites 1, 2 and 5 between mammalian and fungal CYP51, and it is likely that these locations are responsible for conferring selectivity for sterol metabolism (Yoshida et al., 1997). Before the sequences of fungal and human CYP51 were known, this enzyme was identified as an antifungal therapeutic target that could be inhibited by many

imidazole, triazole (Vanden Bossche et al., 1987; Vanden Bossche et al., 1995; Hartman and Sanglard, 1997; Kelly et al., 1997) and non-azole compounds (Aoyama et al., 1983; Yoshida and Aoyama, 1985; Aoyama et al., 1987; Gebhardt et al., 1994; Hartman and Sanglard, 1997). Many of these marketed compounds are specific towards a single fungal species while others have widespread application (Hartman and Sanglard, 1997). The selectivity of these antifungals is also variable, with some exhibiting no interaction with the mammalian enzyme. Many of these azole antifungals are also potent inhibitors of other mammalian P450s involved in drug metabolism and there is thus the potential for clinically significant drug-drug interactions when co-administered with substrates for the same enzymes (Strolin Benedetti and Bani, 1998).

There have been many studies utilizing azole, oxysterol and mechanism-based inactivator-type inhibitors of fungal or mammalian CYP51 (Trzaskos et al., 1986; Frye et al., 1993; Trzaskos et al., 1993; Frye et al., 1994; Trzaskos et al., 1995). In addition, the purification (Sonoda et al., 1993) and expression of human CYP51 has allowed the determination of its regulation by oxysterols (Stromstedt et al., 1996). However, due to the membrane-bound nature of mammalian P450s, there is as yet no crystal structure for human CYP51. Therefore, our understanding of the structural requirements of the human CYP51 active site are limited to homology models constructed using various bacterial P450s (Ishida et al., 1988; Tuck et al., 1991; Tuck et al., 1992; Tafi et al., 1996; Talele et al., 1997; Holtje and Fattorusso, 1998; Lewis et al., 1999) including *M. tuberculosis* CYP51 (Matsuura et al., 2005; Rupp et al., 2005), and the crystal structure of *M. tuberculosis* CYP51 (Podust et al., 2001).

There have also been few quantitative structure activity relationship (QSAR) models of CYP51 to date and they have dealt exclusively with the fungal CYP51s (Tafi et al., 1996; Fujita, 1997). The utility of more classical QSAR has also been reviewed for the production of azole-

type agricultural fungicides (Fujita, 1997). However, approaches towards modeling the common features of inhibitors of other human P450s have been widely shown using a Catalyst™ pharmacophore approach (Ekins et al., 2001), comparative molecular field analysis (CoMFA, (Jones et al., 1996)), and other QSAR methods (Ekins et al., 2003). These techniques have also been used to predict a test-set of molecules excluded from the training set (Ekins et al., 1999).

Recently a series of dual-acting hypoglycemic and hypocholesterolemic agents was found to inhibit glycogen phosphorylase and human CYP51 (Harwood et al., 2005). The prototype of this series, CP-320626, inhibited glycogen phosphorylase and human CYP51 with IC_{50}'s of 155 nM and 4 μM respectively, reduced glycogenolysis and cholesterolgenesis in cultured cells, and lowered plasma glucose and plasma cholesterol in experimental animals (Harwood et al., 2005). In order to understand the characteristics of these CP-320626 related CYP51 inhibitors and other inhibitors of this human CYP51 enzyme, we have used a computational approach to produce a predictive Catalyst™ pharmacophore. This model was constructed using a training set of structurally diverse commercially available molecules and CP-320626-related CYP51 inhibitors with varying IC_{50} values. The validity of the predictions made by this model was then evaluated using test sets of molecules not in the training set. These test sets contained both commercially available molecules and structurally diverse CP-320626-related CYP51 inhibitors for which *in vitro* data were subsequently generated.

Materials and Methods

Materials. Human cytochrome P450 reductase was obtained from Panvera (now Invitrogen, Madison, WI). Rat microsomal lipid was prepared as described by Sundin *et al.* (Sundin et al., 1987). Triarimol, CP-320626 and all other related CYP51 inhibitors denoted as A-P and 1-48 (see Supplemental Table 1 for structures) in the tables were synthesized as described previously (Hoover et al., 1998; Martin et al., 1998; Rath et al., 2000; Treadway et al., 2001; Harwood et al., 2005; Yu et al., 2006) and in the patents cited in these publications. Lovastatin was purchased from Calbiochem (La Jolla, CA). Azaconazole, itraconazole and terconazole were obtained from Research Diagnostics Inc. (Flanders, NJ). Sulphaphenazole was purchased from Gentest Corp. (now BD Gentest, Woburn, MA). Dioleoyl phosphatidyl choline (DOPC), lanosterol (97 % pure), ergosterol and all other chemicals were obtained from Sigma (St. Louis, MO) or Steraloids Inc, (Newport, RI).

CYP51 Lanosterol Demethylase Assay. Human CYP51 expressed in Topp 3 cells was partially purified using the method of Stromstedt (Stromstedt et al., 1996). Protein concentrations were measured using a BCA Protein Assay kit (Pierce Chemical, Rockford, Ill.) with bovine serum albumin as a standard as described by the manufacturer. Cytochrome P450 content was measured by the method of Omura and Sato (Omura and Sato, 1964). Initial rate conditions for the formation of 4,4-dimethylcholesta-8,14,24-trien-3β-ol (triene) were determined in preliminary studies with the CYP51 reconstitution system. Briefly, 25 μL of lanosterol (1 mM, suspended in a mixture of 50/50 tyloxapol / acetone, DOPC micelles (5 mg/ml), methanol, and 100 mM potassium phosphate buffer, pH 7.4) was added to tubes to provide a final lanosterol concentration of 50 μM (approximate K_m). Inhibitors (ranging from

0.01 to 200 μM in methanol) or methanol (control) were then added to tubes, and the lanosterol / inhibitor mixture was allowed to dry under nitrogen for 10 minutes. To dried substrate and inhibitor tubes, 20 pmol CYP51, 125 pmol human reductase, and 50 μl rat lipid were added and allowed to sit at room temperature for 10-15 minutes for enzyme reconstitution. Buffer (100 mM potassium phosphate, pH 7.4, with 20% glycerol, 0.1 mM DTT, 0.1 mM EDTA, and 0.5 mM potassium cyanide) was added to tubes after the reconstitution period for a final incubation volume of 0.5 ml. Tubes were preincubated for 2 minutes at 37^0 C and the reaction was initiated by the addition of 50 μl NADPH regenerating system (final incubation concentration; 10 mM $MgCl_2$, 0.54 mM NADP, 6.2 mM DL-Isocitric Acid, 0.5 U/ml Isocitric Dehydrogenase). Reactions were terminated at 60 min with the addition of 25 μl ergosterol (1 mg/ml in ethyl acetate), followed by extraction with 5 ml ethyl acetate. Tubes were then vortexed before centrifugation followed by removal of 3-4 ml of supernatant and transfer to fresh tubes and evaporation under nitrogen at 50 ^{o}C. The evaporated samples were reconstituted in 150 μl mobile phase, and 25-50 μl was injected onto the HPLC system (see below).

Triene formation was determined using a modification of the method of Strömstedt (Stromstedt et al., 1996). Briefly, triene metabolite and ergosterol were separated on a Waters Novapak C18 column (4.0 μM; 150 mm X 3.9 mm, Bedford, MA) with a mobile phase consisting of methanol:acetonitrile:HPLC grade water (45:45:10), at a flow rate of 1.5 ml/min. The triene and ergosterol were monitored by UV detection at 248 nm using a SpectroMonitor variable wavelength detector (LDC Analytical, Riviera Beach, FL) and the Multichrom™ data acquisition system (Version. 2.11, Fisons Instruments, Beverly, MA) was used for data

collection, analysis and reporting. Approximate retention times for triene metabolite and ergosterol were 25 and 30 minutes, respectively.

Interpretation of CYP51 lanosterol demethylase assay results. The percent inhibition of triene formation with methanol controls was determined with each inhibitor at 3-6 concentrations in triplicate and the average was used as described previously (Harwood et al., 2005). The IC_{50} was calculated from a graph of percent CYP51 activity remaining vs. inhibitor concentration using Deltagraph (Version 4.0, Monterey, CA).

Molecular Modeling. The computational molecular modeling studies were carried out using a Silicon Graphics Octane workstation and based on a pharmacophore methodology previously described for other CYPs (Ekins et al., 1999; Ekins et al., 2001). The pharmacophore method described below represents the features on the ligands used and cannot be related easily to features in the protein binding site. This method has also been applied to other proteins of relevance to absorption, distribution, metabolism, excretion and toxicity (Ekins and Swaan, 2004). The receptor surface modeling method also described below attempts to provide information relating to the volume requirements of the enzyme active site for the heme and non-heme binding compounds with highest affinity.

Modeling with Catalyst™. The 3-D structures of CYP51 inhibitors from the present study or literature data sets were built interactively using Catalyst™ version 4.0 (Accelrys, San Diego, CA). The number of conformers generated for each inhibitor was limited to a maximum of 255 with an energy range of 0 to 20 kcal/mol. A training set of 26 molecules was selected and used to build the pharmacophore (Table 1). Ten hypotheses were generated using these conformers for each of the molecules and IC_{50} values generated after selection of the following features for the inhibitors: hydrogen bond donor, hydrogen bond acceptor, hydrophobic, positive

DMD Fast Forward. Published on December 28, 2006 as DOI: 10.1124/dmd.106.013888
This article has not been copyedited and formatted. The final version may differ from this version.

ionizable and ring aromatic. After assessing all 10 hypotheses generated, the lowest energy cost hypothesis was considered the best.

The goodness of the structure activity correlation was estimated by means of the correlation coefficient r-value. Catalyst™ also calculates the total energy cost of the generated pharmacophores from the deviation between the estimated activity and the observed activity, combined with the complexity of the hypothesis (i.e. the number of pharmacophore features). A null hypothesis is additionally calculated which presumes that there is no relationship in the data and that experimental activities are normally distributed about their mean. Hence, the greater the difference between the energy cost of the generated hypothesis and the energy cost of the null hypothesis, the less likely it is that the hypothesis reflects a chance correlation. This criteria is then used as an assessment of the pharmacophore model selected.

Catalyst™ CYP51 pharmacophore validation using test sets of IC_{50} values. Two test sets of 19 commercially available molecules and 48 proprietary compounds, respectively were subjected to the fast-fit algorithm for the Catalyst™ hypothesis in order to predict a IC_{50} value. None of these molecules was included in the initial training set for the CYP51 IC_{50} pharmacophore. The fast fit algorithm refers to the method of finding the optimum fit of the substrate to the hypothesis among all the conformers of the molecule without performing an energy minimization on the conformers of the molecule (Catalyst™ tutorials release 3.0, Accelrys, San Diego, CA.). The computational predictions derived using the fit to the CYP51 Catalyst™ pharmacophore were compared to the observed *in vitro* values. We selected an acceptable arbitrary cut-off for potency of inhibition as accepted less than or equal to 10 μM.

Catalyst™ CYP51 pharmacophore validation using permuting of activity data. The statistical significance of the pharmacophore hypothesis utilized was tested by permuting

(randomizing) the structures and the activities and then repeating the Catalyst™ hypothesis generation procedure ten times.

Modeling with Cerius^2 ™. The 3-D structures of CYP51 inhibitors generated using Catalyst™ described previously were imported into Cerius^2 ™ (Accelrys, San Diego, CA). Inhibitors with an IC_{50} less than or equal to 10 μM were selected and a receptor surface model (Hahn and Rogers, 1995) was generated. Additional molecules were then fitted to this model in order to discover which features were outside of the volume occupied by the active molecules.

DMD Fast Forward. Published on December 28, 2006 as DOI: 10.1124/dmd.106.013888
This article has not been copyedited and formatted. The final version may differ from this version.

RESULTS

CYP51 in vitro inhibition data. Partially purified CYP51 was characterized for protein and carbon monoxide-difference spectra (data not shown). Total P450 was determined as 0.22 nmol/mg protein. The assay conditions were also developed to provide optimal lanosterol turnover using a final ratio of P450:reductase of 1:6. The K_m determined for lanosterol with the reconstituted human CYP51 was approximately 30 μM (data not shown), in agreement with previously determined values (Lamb et al., 1998). Using a standard concentration of 50 μM lanosterol, 93 commercially available molecules including the competitive inhibitor CP-320626 (Harwood et al., 2005) and related CYP51 inhibitors were screened in the IC_{50} assay (Tables 1-3).

Catalyst ^{TM} CYP51 pharmacophore model. Catalyst™ utilizes a collection of molecules with inhibitory activity over multiple orders of magnitude for the enzyme of interest, in order to construct a model of the structural features (pharmacophore) necessary for interaction of the molecules with the active site of the enzyme. The resultant pharmacophore hypotheses explain the variability of the potency of inhibition with respect to the geometric localization of these features of the molecules. The IC_{50} values for structurally diverse inhibitors of CYP51 generated in this study cover over 3 orders of magnitude (0.13 μM to >200 μM, Table 1). These values were used to build a pharmacophore, with the lowest energy model yielding 4 structural features (Figure 1) necessary for inhibitor binding to the active site of CYP51: 1 hydrophobe, 1 hydrogen bond acceptor and 2 ring aromatic features (additional hydrophobes). The Catalyst™ pharmacophore demonstrated a good correlation of observed versus estimated IC_{50} values ($r = 0.92$, Figure 2).

The total energy cost of the hypothesis (117.3) and the null hypothesis (154.1) suggest that the model was significant as the difference was sizeable. Permuting the training set molecule structures with activities can be used to provide further evidence that the model is statistically reliable (Ekins et al., 1999). After permuting the hypothesis 10 times the mean r value decreased considerably to 0.32 and mean energy cost difference increased to 148.7, almost identical to the null hypothesis value.

Catalyst™ CYP51 pharmacophore validation using test sets of IC_{50} values. After constructing the Catalyst™ 3D-QSAR model for a training set of 26 IC_{50} values generated by this laboratory *in vitro* (Table 1), the model was used to predict IC_{50} values of a test set of 19 commercially available molecules for which in vitro IC_{50} values were also generated (Table 2) and not included in the initial Catalyst™ model. In 16 cases the IC_{50} values were correctly predicted to be either active (IC_{50} < 10 μM) or inactive molecules (IC_{50} >10 μM). The poorly predicted molecules were made up of 5.3 % false negatives (n = 1, bifonazole) and 10.5 % false positives (n = 2, Triarimol and Azaconazole).

A second test set of IC_{50} values was composed of 48 CP-320626 related CYP51 inhibitors of which 38 were correctly predicted using the Catalyst™ 3D-QSAR model following the criteria as described above (Table 3). The poorly predicted molecules were made up of 4.2 % false negatives (n = 2, molecules 1, 37) and 16.6 % false positives (n = 8, molecules 7, 12, 38, 39, 44, 45, 46, 47).

Modeling with Cerius^2 ™. Fifteen molecules with *in vitro* IC_{50} values < 10 μM produced a volume using the receptor surface model software present in Cerius^2 ™ (Figure 3A). When fluconazole, an inhibitor with a low affinity for human CYP51 was fitted to this model, part of the molecule lies outside of the volume (Figure 3B).

DISCUSSION

In humans, beyond its obvious role in cholesterol and steroid hormone biosynthesis (Trzaskos et al., 1986), the physiological roles of CYP51 in, for example spermatogenesis and oogenesis (Stromstedt et al., 1998), are poorly defined. In addition, inhibition of cholesterol biosynthesis through inhibition of mammalian CYP51 results in an increase in cellular lanosterol concentrations (Miettinen, 1988), the consequences of which remain poorly defined. Further, the poor specificity of most current mammalian CYP51 inhibitors for CYP51 versus steroidogenic or drug-metabolizing P450s (Hartman and Sanglard, 1997; Strolin Benedetti and Bani, 1998) implies that molecules aimed at other therapeutic targets should preferably avoid interaction with this enzyme.

Since there is no crystal structure for the human membrane-bound CYP51, alternative techniques must be considered to understand whether a novel molecule will bind to it. It is possible, however, to begin to understand the specificity of an enzyme without possessing information regarding its crystal structure. The most widely used computational method for modeling in the cytochrome P450 field is homology modeling based on crystallized bacterial CYPs. The initial models of the active site for CYP51 from S. cerevisiae and an inactive mutant (Ishida et al., 1988) were constructed using alignment with P450cam. Using these, novel substrate analogs were developed as competitive inhibitors for this enzyme (Tuck et al., 1991). The formation of a fungal CYP51 biphenyl-iron complex also yielded information as to the approximate height of the cavity (10Å) above the porphyrin ring in the active site (Tuck et al., 1992). Further work studying the I-helix of the fungal CYP51 with lanosterol has shown that Gly-310 is an important residue, although interactions at His-317 and Met-313 may also occur (Vanden Bossche et al., 1995). It has been suggested that whereas ketoconazole and itraconazole

have multiple interactions with the CYP51 I-helix, fluconazole has fewer and may result in its lower antifungal activity (Vanden Bossche and Koymans, 1998). Comparative homology models have identified differences in the active sites of C. albicans and S. cerevisiae (Boscott and Grant, 1994) in agreement with earlier work (Yoshida and Aoyama, 1987). When the human CYP51 I-helix sequence is aligned with those from C. albicans and S. cerevisiae (Vanden Bossche and Koymans, 1998) there are 6 amino acids which are different between the fungal and the human P450s. It is therefore likely that the surface volume of inhibitors for fungi and human CYP51 could be markedly different due to the alteration in the active site caused by these amino acid substitutions. Numerous studies have used homology modeling and docking for CYP51 to show: lanosterol hydrogen bonding interactions (Holtje and Fattorusso, 1998), triazole and azole inhibitors interacting with the hydrophobic active site and the heme iron (Talele et al., 1997) and functional group modifications that alter enzyme-inhibitor interactions (Tsukuda et al., 1998). CYP51 homology models have been used in de novo design (Ji et al., 2000) and in understanding azole binding to human and crystallized M. tuberculosis CYP51 enzymes (Matsuura et al., 2005; Rupp et al., 2005). The latter study indicated that the human enzyme may have a larger and differently shaped active site cavity due to the replacement of Phe-255 with Leu-310 (Matsuura et al., 2005; Rupp et al., 2005).

Although there are data sets in the literature describing the fungicidal activity of CYP51 inhibitors (Stehmann and de Waard, 1995), there is little information relating to human disease. The present study has described to our knowledge the first 3D-QSAR relationship using *in vitro* data for inhibitors of human CYP51. By using 26 structurally diverse molecules with a range of inhibitory activity, we constructed a predictive pharmacophore model that was used to score the activity of test molecules and predict whether new chemical entities might interact with this

enzyme. The model for the data set generated in this study suggested a pharmacophore with four features, indicating the predominance of hydrophobic features (Figure 1) in agreement with previous reports (Matsuura et al., 2005; Rupp et al., 2005), and a high correlation ($r = 0.92$, Figure 2) between predicted and observed IC_{50} values.

One of the best ways to test the validity of a 3D-QSAR is to predict the activity of molecules excluded from the training set and then compare these to observed values. In addition to prospectively assessing many proprietary compounds, several commercially available molecules were evaluated *in vitro* as they had either important endogenous roles (cholesterol, arachidonic acid, progesterone, pregnenolone and anandamide), were known CYP substrates (erythromycin, tolbutamide, lovastatin, chlorpropamide, propafenone) or were known CYP inhibitors (sulphaphenazole, fluconazole, azaconazole, econazole, bifonazole, terconazole, itraconazole, triarimol and sulfinpyrazone). It was thought that these molecules would provide a structurally diverse test set in order to validate the pharmacophore constructed from a similarly structurally diverse training set including heme-binding azoles and non heme-binding CP-320626-related compounds (Harwood et al., 2005). *In vitro* IC_{50} values were generated for CYP51 inhibition for 19 commercially available molecules. Sixteen of the 19 (84 %) molecules fulfilled the criterion (Table 2). Non heme-binding CP-320626-related CYP51 inhibitors were also successfully predicted using the same pharmacophore model with an approximate 80 % prediction rate (Table 3). These results suggest that the CYP51 pharmacophore has utility for both classification of novel molecules that are either known heme binders or non-heme binders with an acceptable level of accuracy for early screening.

By aligning the most potent CYP51 inhibitors (azoles and CP320626-related compounds) with the pharmacophore it was possible to generate a receptor surface model of

their volume. The receptor surface model of these active inhibitors forms an elongated shape (Figure 3A), not too dissimilar to that of lanosterol and the volume generated by Rupp et al., (Rupp et al., 2005). This receptor surface model can also be used to explain the apparent lack of inhibitory activity towards human CYP51 by inactive molecules, by first mapping them to the pharmacophore and then placing them inside this receptor surface model. Features outside of the volume could suggest poor steric interactions within the active site of the enzyme that would be unfavorable for binding and therefore inhibition. As an example, we have fitted fluconazole to the pharmacophore and shown that a triazole ring is outside of the surface volume generated by the active compounds (Figure 3B). This may explain the lack of potency of fluconazole towards the human CYP51 but subsequent activity towards the fungal P450. Indeed this is in agreement with a recent study that has also shown that fluconazole is considerably less active than ketoconazole with human CYP51 with K_d values of 120 μM and 8 μM, respectively. The differential potency between these two compounds may also be in part because fluconazole possesses a hydrophilic triazole and hydroxyl groups that would decrease affinity for the hydrophobic binding site relative to the more hydrophobic ketoconazole (Matsuura et al., 2005).

The computational techniques described and applied in this paper may allow elucidation of areas within the human CYP51 active site that can be targeted by *directed* synthesis to enable production of more selective antifungal agents. Similarly, if human CYP51 is pursued as a therapeutic target, for example in cancer (Downie et al., 2005; Kumarakulasingham et al., 2005), this pharmacophore model enables mining of compound databases for inhibitors and may help to understand the affinity of inhibitors for the human CYP51 active site. Specific inhibitors of human CYP51 (Harwood et al., 2005) might also be applicable, for example, as agents for lipid lowering, either alone or in combination with other agents (e.g. HMG CoA reductase inhibitors)

currently marketed and / or in development (Harwood and Hamanaka, 1998) for use as therapeutic intervention in areas with substantial medical need such as coronary heart disease, obesity and diabetes.

While the pharmacophore technique could represent an approach for identifying modulators of human CYP51, possibly by database screening, we have taken the same approach with *in vitro* data for antifungal activity (Tafi et al., 1996), to create a second pharmacophore for fungal CYP51 (data not shown). Therefore it is possible to differentiate between the human and fungal CYP51 enzymes *in silico* to develop selective modulators of this enzyme across phyla., The publication of X-ray structures of CYP51 in M. tuberculosis with bound inhibitors (Podust et al., 2001) suggests we will require selective inhibitors if we are to capitalize on CYP51 as a therapeutic target; the human CYP51 pharmacophores may allow this in combination with the protein models (de Groot and Ekins, 2002).

In conclusion, this study has described a large number of molecules tested as potential CYP51 inhibitors and has enabled the identification of non-azoles with low μM potency. These molecules have been used to build and test the first 3D-QSAR for human CYP51, which can be used to predict the inhibitory potential of other molecules towards this enzyme. We suggest that this CYP51 pharmacophore may be used to garner information regarding the interactions with the active site of this P450 and visually describe the selectivity of antifungal agents. This model could also enable rapid discovery of further modulators of this enzyme for therapeutic use.

ACKNOWLEDGEMENT

We gratefully acknowledge Professor Michael R Waterman (Department of Biochemistry, Vanderbilt University School of Medicine, Nashville, TN) for supplying clones expressing recombinant CYP51, Ms. Joanne Jeffries-Griffor (Molecular Sciences, Pfizer Global Research and Development.) for partial purification of CYP51 from these clones, and Dr. Patrick Dorr, Pfizer, Sandwich UK for supplying several of the compounds evaluated in these studies.

REFERENCES

Aoyama Y, Noshiro M, Gotoh O, Imaoka S, Funae Y, Kurosawa N, Horiuchi T and Yoshida Y (1996) Sterol 14-demethylase P450 (P45014DM) is one of the most ancient and conserved P450 species. *Journal of Biochemistry (Tokyo)* **119:**926-933.

Aoyama Y, Yoshida Y, Hata S, Nishino T and Katsuki H (1983) Buthiobate: a potent inhibitor for yeast cytochrome P-450 catalyzing 14 alpha-demethylation of lanosterol. *Biochem Biophys Res Commun* **115:**642-647.

Aoyama Y, Yoshida Y, Sonoda Y and Sato Y (1987) 7-Oxo-24,25-dihydrolanosterol: A novel lanosterol 14alpha-demethylase (P-450(14DM)) inhibitor which blocks electron transfer to the oxyferro intermediate. *Biochim. Biophys. Acta, Ser. Lipids Lipid Metab.* **922:**270-277.

Boscott PE and Grant GH (1994) Modeling cytochrome P450 14 alpha demethylase (Candida albicans) from P450cam. *J Mol Graph* **12:**185-192, 195.

Chan JR, Phillips LJ, 2nd and Glaser M (1998) Glucocorticoids and progestins signal the initiation and enhance the rate of myelin formation. *Proc Natl Acad Sci U S A* **95:**10459-10464.

de Groot MJ and Ekins S (2002) Pharmacophore modeling of cytochromes P450. *Adv Drug Del Rev* **54:**367-383.

Downie D, McFadyen MC, Rooney PH, Cruickshank ME, Parkin DE, Miller ID, Telfer C, Melvin WT and Murray GI (2005) Profiling cytochrome P450 expression in ovarian cancer: identification of prognostic markers. *Clin Cancer Res* **11:**7369-7375.

Ekins S, Berbaum J and Harrison RK (2003) Generation and validation of rapid computational filters for CYP2D6 and CYP3A4. *Drug Metab Dispos* **31:**1077-1080.

Ekins S, Bravi G, Ring BJ, Gillespie TA, Gillespie JS, VandenBranden M, Wrighton SA and Wikel JH (1999) Three dimensional-quantitative structure activity relationship (3D-QSAR) analyses of substrates for CYP2B6. *J Pharm Exp Ther* **288:**21-29.

Ekins S, de Groot M and Jones JP (2001) Pharmacophore and three dimensional quantitative structure activity relationship methods for modeling cytochrome P450 active sites. *Drug Metab Dispos* **29:**936-944.

Ekins S and Swaan PW (2004) Development of computational models for enzymes, transporters, channels and receptors relevant to ADME/TOX. *Rev Comp Chem* **20:**333-415.

Frye LL, Cusack KP and Leonard DA (1993) 32-Methyl-32-Oxylanosterols - Dual-Action Inhibitors of Cholesterol-Biosynthesis. *Journal of Medicinal Chemistry* **36:**410-416.

Frye LL, Cusack KP, Leonard DA and Anderson JA (1994) Oxolanosterol Oximes - Dual-Action Inhibitors of Cholesterol-Biosynthesis. *Journal of Lipid Research* **35:**1333-1344.

Fujita T (1997) Recent success stories leading to commercializable bioactive compounds with the aid of traditional QSAR procedures. *Quant Struct Act Relat* **16:**107-112.

Gebhardt R, Beck H and Wagner KG (1994) Inhibition of cholesterol biosynthesis by allicin and ajoene in rat hepatocytes and HepG2 cells. *Biochim. Biophys. Acta Lipids Lipid Metab.* **1994:**57-62.

Hahn M and Rogers D (1995) Receptor Surface Models 2. Application to quantitative structure-activity relationships studies. *Journal of Medicinal Chemistry* **38:**2091-2102.

Hartman PG and Sanglard D (1997) Inhibitors of ergosterol biosynthesis as antifungal agents Recent success stories leading to commercializable bioactive compounds with the aid of traditional QSAR procedures. *Current Pharmaceutical Design* **3:**177-208.

Harwood H and Hamanaka E (1998) Emerging Drugs. **3:**147-172.

Harwood HJ, Jr., Petras SF, Hoover DJ, Mankowski DC, Soliman VF, Sugarman ED, Hulin B, Kwon Y, Gibbs EM, Mayne JT and Treadway JL (2005) Dual-action hypoglycemic and hypocholesterolemic agents that inhibit glycogen phosphorylase and lanosterol demethylase. *J Lipid Res* **46:**547-563.

Hiroi T, Imaoa S and Funae Y (1998) Dopamine formation from tyramine by CYP2D6. *Biochem Biophys Res Comm* **249:**838-843.

Holtje HD and Fattorusso C (1998) Construction of a model of the Candida albicans lanosterol 14-alpha- demethylase active site using the homology modelling technique. *Pharmaceutica Acta Helvetiae* **72:**271-277.

Hoover DJ, Lefkowitz-Snow S, Burgess-Henry JL, Martin WH, Armento SJ, Stock IA, McPherson RK, Genereux PE, Gibbs EM and Treadway JL (1998) Indole-2-carboxamide inhibitors of human liver glycogen phosphorylase. *J Med Chem* **41:**2934-2938.

Ishida N, Aoyama Y, Hatanaka R, Oyama Y, Imajo S, Ishiguro M, Oshima T, Nakazato H, Noguchi T, Maitra US, Mohan VP, Sprinson DB and Yoshida Y (1988) A single amino acid substitution converts cytochrome P450(14DM) to an inactive form, cytochrome P450(SG1): Complete primary structures deduced from cloned DNAs. *Biochem. Biophys. Res. Commun.* **155**: 317- 323.

Ji H, Zhang W, Zhou Y, Zhang M, Zhu J, Song Y, Lu J and Zhu J (2000) A three dimensional model of lanosterol 14a-demethylase of candida albicans and its interaction with azole antinfungals. *J Med Chem* **43:**2493-2505.

Jones JP, He M, Trager WF and Rettie AE (1996) Three-dimensional quantitative structure-activity relationship for inhibitors of cytochrome P4502C9. *Drug Metab Dispos* **24:**1-6.

Kelly SL, Lamb DC, Baldwin BC, Corran AJ and Kelly DE (1997) Characterization of Saccharomyces cerevisiae CTP61, sterol Delta22- desaturase, and inhibition by azole antifungal agents. *Journal of Biological Chemistry* **272:**9986-9988.

Kumarakulasingham M, Rooney PH, Dundas SR, Telfer C, Melvin WT, Curran S and Murray GI (2005) Cytochrome p450 profile of colorectal cancer: identification of markers of prognosis. *Clin Cancer Res* **11:**3758-3765.

Lamb DC, Kelly DE and Kelly SL (1998) Molecular diversity of sterol 14-alpha-demethylase substrates in plants, fungi and humans. *FEBS Letters* **425:**263-265.

Lewis DFV, Wiseman A and Tarbit MH (1999) Molecular modelling of lanosterol 14a-demethylase (CYP51) from *Sachharomyces cerevisiae* via homology with CYP102, a unique bacterial cytochrome P450 isoform: Quantitative Structure-activity relationships (QSARs) within two related series of antifungal azole derivatives. *J Enzyme Inhibition* **14:**175-192.

Martin WH, Hoover DJ, Armento SJ, Stock IA, McPherson RK, Danley DE, Stevenson RW, Barrett EJ and Treadway JL (1998) Discovery of a human liver glycogen phosphorylase inhibitor that lowers blood glucose in vivo. *Proc Natl Acad Sci U S A* **95:**1776-1781.

Matsuura K, Yoshioka S, Tosha T, Hori H, Ishimori K, Kitagawa T, Morishima I, Kagawa N and Waterman MR (2005) Structural diversities of active site in clinical azole-bound forms between sterol 14alpha-demethylases (CYP51s) from human and Mycobacterium tuberculosis. *J Biol Chem* **280:**9088-9096.

Miettinen TA (1988) Cholesterol metabolism during ketoconazole treatment in man. *J Lipid Res* **29:**43-51.

Nelson DR, Koymans L, Kamataki T, Stegeman JJ, Feyereisen R, Waxman DJ, Waterman MR, Gotoh O, Coon MJ, Estabrook RW, Gunsalus IC and Nebert DW (1996) P450 superfamily: update on new sequences, gene mapping, accession numbers and nomenclature. *Pharmacogenetics* **6:**1-42.

Omura T and Sato R (1964) The Carbon Monoxide-Binding Pigment of Liver Microsomes. I. Evidence for Its Hemoprotein Nature. *J Biol Chem* **239:**2370-2378.

Podust LM, Poulos TL and Waterman MR (2001) Crystal structure of cytochrome P450 14alpha -sterol demethylase (CYP51) from Mycobacterium tuberculosis in complex with azole inhibitors. *Proc Natl Acad Sci U S A* **98:**3068-3073.

Rath VL, Ammirati M, Danley DE, Ekstrom JL, Gibbs EM, Hynes TR, Mathiowetz AM, McPherson RK, Olson TV, Treadway JL and Hoover DJ (2000) Human liver glycogen phosphorylase inhibitors bind at a new allosteric site. *Chem Biol* **7:**677-682.

Rozman D, Stromstedt M, Tsui LC, Scherer SW and Waterman MR (1996) Structure and mapping of the human lanosterol 14alpha-demethylase gene (CYP51) encoding the cytochrome P450 involved in cholesterol biosynthesis; comparison of exon/intron organization with other mammalian and fungal CYP genes. *Genomics* **38:**371-381.

Rupp B, Raub S, Marian C and Holtje HD (2005) Molecular design of two sterol 14alpha-demethylase homology models and their interactions with the azole antifungals ketoconazole and bifonazole. *J Comput Aided Mol Des* **19:**149-163.

Sonoda Y, Endo M, Ishida K, Sato Y, Fukusen N and Fukuhara M (1993) Purification of a human cytochrome P-450 isozyme catalyzing lanosterol 14 alpha-demethylation. *Biochim Biophys Acta* **1170:**92-97.

Stehmann C and de Waard M (1995), Relationship between chemical structure and biological activity of triazole fungicides against Botrytis Cinerea. *Pestic Sci* **44:**183-195.

Strolin Benedetti M and Bani M (1998), in: *Microsomes and Drug Oxidations*, pp S17-12, Montpelier, France.

Stromstedt M, Rozman D and Waterman MR (1996) The ubiquitously expressed human CYP51 encodes lanosterol 14-alpha-demethylase, a cytochrome P450 whose expression is regulated by oxysterols. *Archives of Biochemistry and Biophysics* **329:**73-81.

Stromstedt M, Waterman MR, Haugen TB, Tasken K, Parvinen M and Rozman D (1998) Elevated expression of lanosterol 14alpha-demethylase (CYP51) and the synthesis of oocyte meiosis-activating sterols in postmeiotic germ cells of male rats. *Endocrinology* **139:**2314-2321.

Sundin M, Warner M, Haaparanta T and Gustafsson JA (1987) Isolation and catalytic activity of cytochrome P-450 from ventral prostate of control rats. *J Biol Chem* **262:**12293-12297.

Tafi A, Anastassopoulou J, Theophanides T, Botta M, Corelli F, Massa S, Artico M, Costi R, Di Santo R and Ragno R (1996) Molecular modeling of azole antifungal agents active against *Candida albicans*. 1. A comparative molecular field analysis study. *J Med Chem* **39:**1227-1235.

Talele TT, Hariprasad V and Kulkarni VM (1997) Docking analysis of a series of cytochrome P-450(14) alpha DM inhibiting azole antifungals. *Drug Des Discov* **15:**181-190.

Treadway JL, Mendys P and Hoover DJ (2001) Glycogen phosphorylase inhibitors for treatment of type 2 diabetes mellitus. *Expert Opin Investig Drugs* **10:**439-454.

Trzaskos J, Kawata S and Gaylor JL (1986) Microsomal enzymes of cholesterol biosynthesis. Purification of lanosterol 14alpha-methyl demethylase cytochrome P-450 from hepatic microsomes. *J. Biol. Chem.* **261:**14651-14657.

Trzaskos JM, Ko SS, Magolda RL, Favata MF, Fischer RT, Stam SH, Johnson PR and Gaylor JL (1995) Substrate-based inhibitors of lanosterol 14 alpha-methyl demethylase: I. Assessment of inhibitor structure-activity relationship and cholesterol biosynthesis inhibition properties. *Biochemistry* **34**: 9670-9676.

Trzaskos JM, Magolda RL, Favata MF, Fischer RT, Johnson PR, Chen HW, Ko SS, Leonard DA and Gaylor JL (1993) Modulation of 3-Hydroxy-3-Methylglutaryl-Coa Reductase By 15-Alpha-Fluorolanost-7-En-3-Beta-Ol - a Mechanism-Based Inhibitor of Cholesterol-Biosynthesis. *Journal of Biological Chemistry* **268:**22591-22599.

Tsukuda T, Shiratori Y, Watanabe M, Ontsuka H, Hattori K, Shirai M and Shimma N (1998) Modeling, synthesis and biological activity of novel antifungal agents (1). *Bioorganic & Medicinal Chemistry Letters* **8:**1819-1824.

Tuck EF, Robinson CH and Silverton JV (1991) Assessment of the active-site requirements of lanosterol 14 alpha -demethylase : evaluation of novel substrate analogues as competitive inhibitors. *Journal of organic chemistry (The)* **56:**1260-1266.

Tuck SF, Aoyama Y, Yoshida Y and Ortiz de Montellano PR (1992) Active site topology of *saccharomyces cerevisae* lanosterol 14α-demethylase (CYP51) and its G310D mutant (Cytochrome P-450_{SG}1). *J Biol Chem* **267:**13175-13179.

Vanden Bossche H and Koymans L (1998) Cytochromes P450 in fungi. *Mycoses* **41:**32-38.

Vanden Bossche H, Koymans L and Moereels H (1995) P450 inhibitors of use in medical treatment: focus on mechanisms of action. *Pharmacol Ther* **67:**79-100.

Vanden Bossche H, Marichal P, Gorrens J, Bellens D, Verhoeven H, Coene M-C, Lauwers W and Janssen PAJ (1987) Interaction of azole derivatives with cytochrome P-450 Isozymes in yeast, Fungi, plants and mammalian cells. *Pestic Sci* **21:**289-306.

Waterman MR and Lepesheva GI (2005) Sterol 14 alpha-demethylase, an abundant and essential mixed-function oxidase. *Biochem Biophys Res Commun* **338:**418-422.

Wrighton SA, Ring BJ and VandenBranden M (1995) The use of in vitro metabolism techniques in the planning and interpretation of drug safety studies. *Toxicologic Pathology* **23:**199-208.

Yoshida Y and Aoyama Y (1985) Effects of buthiobate, a fungicide, on cytochrome P-450 of rat liver microsomes. *J Pharmacobiodyn* **8:**432-439.

Yoshida Y and Aoyama Y (1987) Interaction of azole antifungal agents with cytochrome P-45014DM purified from Saccharomyces cerevisiae microsomes. *Biochem Pharmacol* **36**.229-235.

Yoshida Y, Noshiro M, Aoyama Y, Kawamoto T, Horiuchi T and Gotoh O (1997) Structural and evolutionary studies on sterol 14-demethylase P450 (CYP51), the most conserved P450 monooxygenase: II. Evolutionary analysis of protein and gene structures. *Journal of Biochemistry (Tokyo)* **122:**1122-1128.

Yu LJ, Chen Y, Treadway JL, McPherson RK, McCoid SC, Gibbs EM and Hoover DJ (2006) Establishment of correlation between in vitro enzyme binding potency and in vivo pharmacological activity: application to liver glycogen phosphorylase a inhibitors. *J Pharmacol Exp Ther* **317:**1230-1237.

FOOTNOTES PAGE

a) Send reprint requests to:

Sean Ekins, D.Sc., ACT LLC, 601 Runnymede Avenue, Jenkintown, PA 19046. Email

ekinssean@yahoo.com

b) Numbered footnotes

[1] Present address: ACT LLC, 601 Runnymede Avenue, Jenkintown, PA 19046.

[2] Present address: Department of Pharmacology, University of Connecticut Health Center, 263 Farmington Av., Farmington, CT 06030, USA.

Figure Legends

Figure 1. The human CYP51 pharmacophore for n = 26 inhibitors generated using Catalyst ™ (see Materials and Methods) illustrating 1 hydrophobe (cyan), 1 hydrogen bond acceptor (green) and 2 ring aromatic features (orange). The inter bond angles and the distances between features are also annotated.

Figure 2. Correlation of observed and estimated inhibition IC_{50} (log units) for the CYP51 Catalyst ™ model. The central line corresponds to the regression of the data; the dashed lines represent the 95% confidence interval for the regression while the outer lines are the 95% confidence interval for the population.

Figure 3. A. Opaque Cerius2™ receptor surface model of active CYP51 inhibitors showing hydrogen bond acceptor regions (blue coloring) - front view. This model was generated with training set molecules with IC_{50} values less than or equal to 10 μM (see Materials and Methods). B. Fluconazole fitted to Cerius2™ receptor surface model (side view) for human CYP51, showing an area of the molecule outside of the surface boundary for this volume (see Materials and Methods).

DMD Fast Forward. Published on December 28, 2006 as DOI: 10.1124/dmd.106.013888
This article has not been copyedited and formatted. The final version may differ from this version.

Table 1. Commercial and CP-320626 analog CYP51 inhibitors used as a Catalyst™ training set

Inhibitor	Structure	Observed CYP51 IC_{50} (μM)*	Estimated CYP51 IC_{50} (μM)*
Clotrimazole	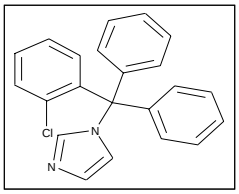	0.13	1.3
Ketoconazole	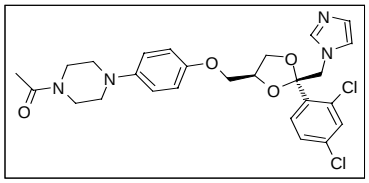	0.19	0.082
Miconazole	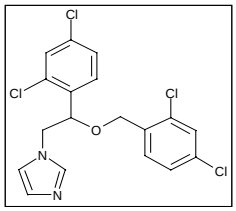	0.2	1.7
Analog A	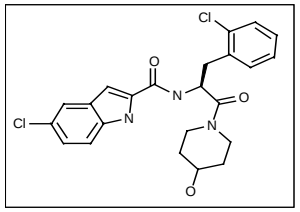	0.3	1.2
Analog B		0.8	2.2

DMD Fast Forward. Published on December 28, 2006 as DOI: 10.1124/dmd.106.013888
This article has not been copyedited and formatted. The final version may differ from this version.

	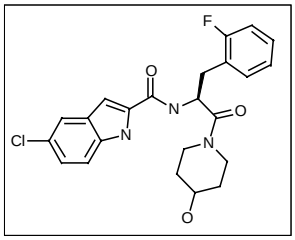		
Analog C		0.91	2
	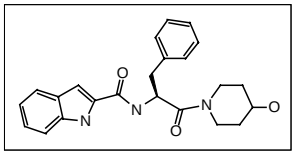		
Analog D		1.3	6.9
	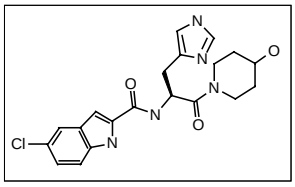		
Analog E		2.5	2.9
	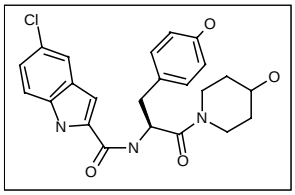		
Analog F		3.1	1.5
	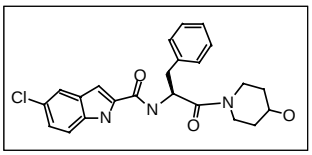		
CP-320626		4.0	2.8
	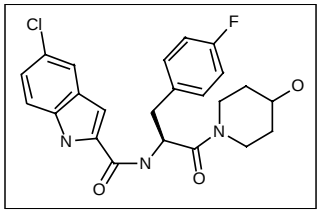		

Analog G	4.5	3.2

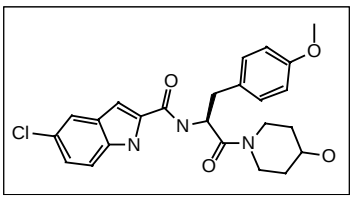

Analog H	9.7	3.5

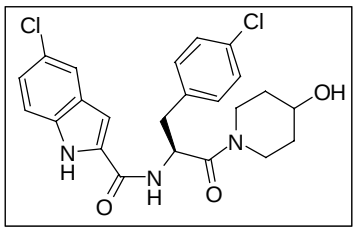

Analog I	26	3.3

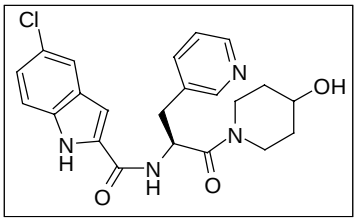

Rifampicin	30	130

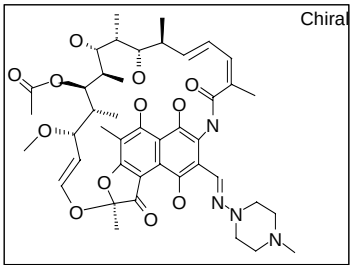

Griseofulvin	50	120

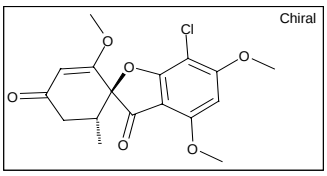

DMD Fast Forward. Published on December 28, 2006 as DOI: 10.1124/dmd.106.013888
This article has not been copyedited and formatted. The final version may differ from this version.

Tolnaftate	50	25

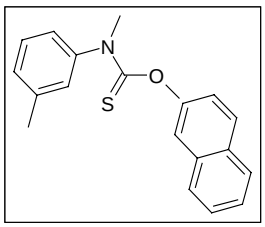

Testosterone	50	160

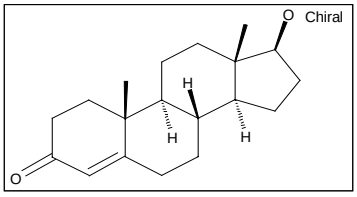

Analog J	75	44

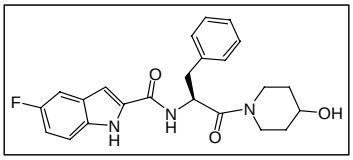

Analog K	100	60

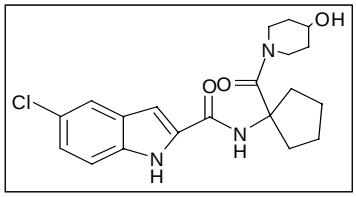

Analog L	100	14

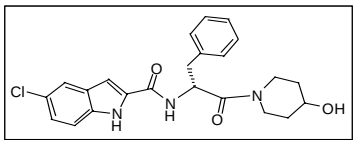

Benzimidazole	>200	150

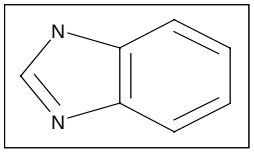

Metronidazole	>200	64
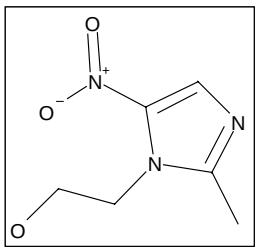		
Methimazole	>200	130
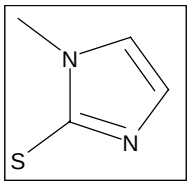		
Analog M	>200	110
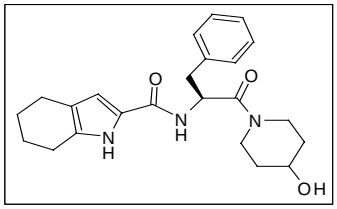		
Analog N	>200	130
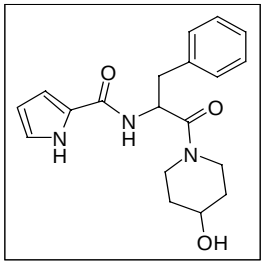		
Analog O	>200	89
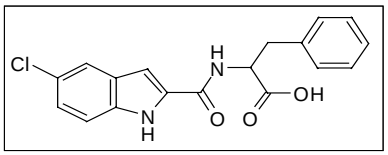		

* Experimental data is the average of triplicate determinations.

Table 2. Observed and predicted IC_{50} values for diverse molecules tested as inhibitors of CYP51 that were fast fit to the Catalyst™ CYP51 pharmacophore

Inhibitor	Observed In vitro IC_{50} (μM)*	Predicted Catalyst™ fast fit IC_{50} (μM)*
Cholesterol	>200	96
Erythromycin	>200	89
Sulphaphenazole	>200	16
Tolbutamide	>200	120
Fluconazole	>200	96
Propafenone	>200	17
Progesterone	>200	92
Arachidonic acid	>200	92
Chlopropamide	>200	92
Anandamide	>200	90
Sulfinpyrazone	>200	93
Triarimol	>10	0.85
Bifonazole	0.342	140
Azaconazole	>10	0.88
Econazole	0.05	0.51

Lovastatin	>200	89
Pregnenolone	>200	98
Terconazole	3	0.43
Itraconazole	3.6	0.82

* Experimental data is the average of triplicate determinations.

DMD Fast Forward. Published on December 28, 2006 as DOI: 10.1124/dmd.106.013888
This article has not been copyedited and formatted. The final version may differ from this version.

Table 3. Observed and predicted IC_{50} values for CP-320626-related analogs tested as inhibitors of CYP51 and fast fit to the Catalyst™ CYP51 pharmacophore (Structures for molecules provided in supplemental Table 1).

CP-320626-related molecules	Observed *in vitro* IC_{50} (μM)*	Predicted Catalyst™ fast fit IC_{50} (μM)*
1	6	43
2	22	91
3	>30	72
4	>30	79
5	3.5	0.91
6	>10	91
7	>10	6
8	>10	90
9	>10	90
10	>10	97
11	>10	52
12	>10	5.8
13	>10	92
14	>10	30
15	>10	91

16	20	91
17	50	95
18	>30	95
19	>30	90
20	14	92
21	5	5.2
22	>30	79
23	>30	42
24	>30	90
25	>10	95
26	>10	93
27	>10	60
28	>10	93
29	>10	91
30	>10	91
31	>10	63
32	>10	39
33	>10	14
34	>10	92
35	1.2	4.8
36	5.7	8.1
37	6.0	43

38	28	1.9
39	>200	1.9
40	>10	26
41	>10	120
42	>10	170
43	>10	29
44	>10	0.46
45	>10	0.51
46	>30	0.39
47	>30	0.41
48	0.7	0.43

* Experimental data is the average of triplicate determinations.

Fig 1

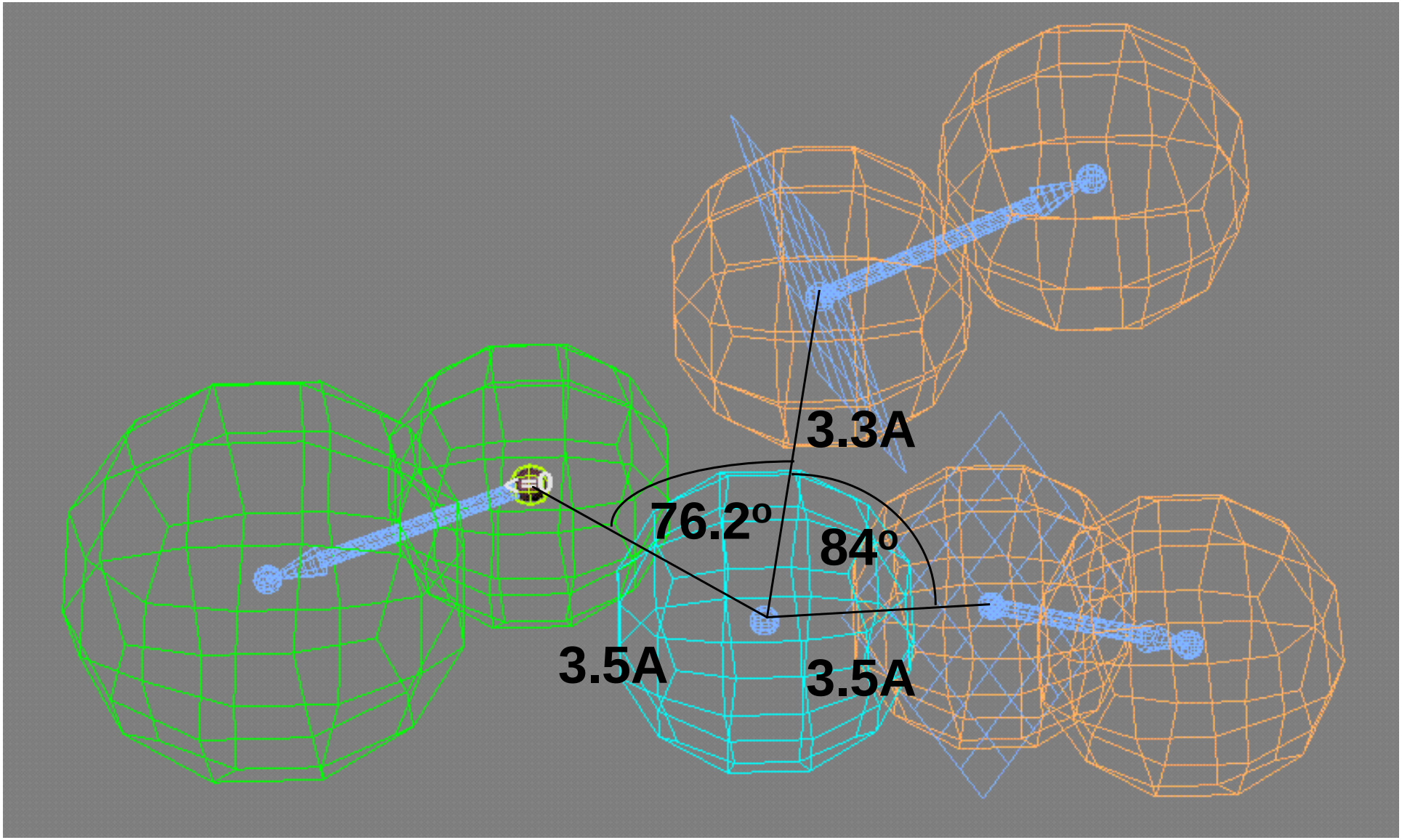

Fig 2

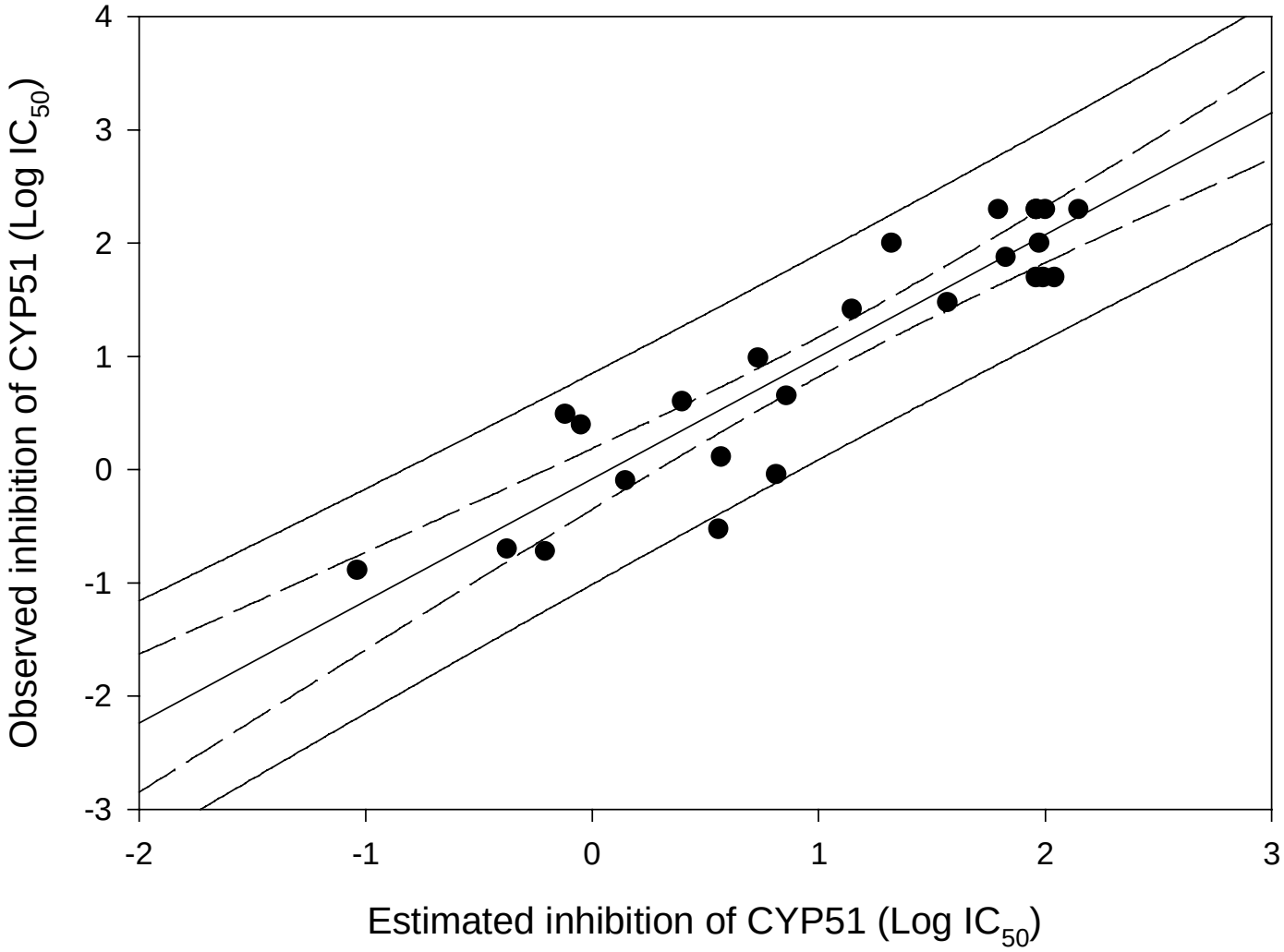

Fig 3

A

B

CORRECTION TO "THREE-DIMENSIONAL QUANTITATIVE STRUCTURE-ACTIVITY RELATIONSHIP ANALYSIS OF HUMAN CYP51 INHIBITORS"

In Table 1 on page 496 of the article above [Ekins S, Mankowski DC, Hoover DJ, Lawton MP, Treadway JL, and Harwood HJ Jr (2007) *Drug Metab Dispos* **35:**493–500], the chemical structure for analog L was inadvertently dropped and replaced with a duplicate of the structure for benzimidazole. The correct structure for analog L appears below.

The online version of this article will be corrected in departure from the print version.

The printer regrets this error and apologizes for any confusion or inconvenience it may have caused.